Probabilistic calibration of the strength reduction factor for the design of rectangular short concrete columns reinforced with FRP bars under eccentric axial loading – Update of ACI 440 rules

Osama Ali, Mohamed Zakaria, Hassen Riahi, David Bigaud

Version of Record: https://www.sciencedirect.com/science/article/pii/S2352710221009542
Manuscript_2987bbae3e58de165e6915738da8807e

Probabilistic calibration of the strength reduction factor for the design of rectangular short concrete columns reinforced with FRP bars under eccentric axial loading – update of ACI 440 rules.

Abstract:
The design of concrete columns reinforced with fibre-reinforced polymer (FRP) bars is currently debatable. The present study proposes a reliability-based approach with the objective of calibrating the optimal strength reduction factor for the design of short rectangular FRP-RC columns under eccentric axial loading according to the ACI-440 guide. The reliability approach relies on a fast hybrid first-order reliability method (FORM)-based response-surface (RS) method. The results of such a hybrid approach have been validated using a Monte Carlo importance sampling (MC-IS) technique. The uncertainty of geometrical, material and loading variables is considered through various dedicated statistical distribution laws. Several design parameters have been considered: load eccentricity, aspect ratio of the concrete section, reinforcement ratio, live to dead load ratio, strength of concrete, and grade of FRP bars. In addition, Top-Bottom and Uniform reinforcement configurations, which are preferred for high- and small-load eccentricities, respectively, are considered. To ensure the generalization of the approach, full combinations between the design parameters are performed, resulting in more than 10^5 structural classes. Thus, calibrated strength reduction factors can cover a wide range of design situations. After demonstrating the possible inappropriateness of ACI-440 rules, the study proposes a novel approach to choose the strength reduction factors based on a quadratic function of the live-to-dead load ratio and load eccentricity. Eventually, the study presents recommendations for the selection of reduction factors distinguishing small and high load eccentricity and concludes with a working example.

Keywords: Fibre Reinforced Polymer bars; short concrete columns; design code; structural reliability analysis; calibration of strength reduction factor.

1. Introduction

Reinforced concrete (RC) members containing conventional steel reinforcing bars often suffer from a decrease in their strength with time due to corrosion, which is inevitable, and sometimes at an early age, especially in coastal and/or industrial zones [1-3]. Corrosion is a common problem in conventional steel materials and cannot be totally prevented throughout the life span of structures. Thus, engineers have been forced to use another type of reinforcement, and in the last two decades, fibre-reinforced polymer (FRP) composite bars have been used as an alternative reinforcement

material in concrete structures since FRPs are noncorrodible materials [4]. Furthermore, use of FRPs could offer more advantages, such as light weight, ease of transportation and fabrication, high static [5] and cyclic [6] strength and durability [7], and even under high temperature [8], compared to conventional steel bars.

Flexural and shear design rules of RC members reinforced with FRP bars are included in several design guidelines or handbooks, such as [9], FIB [10] and ISIS Canada [11]. Currently, most of the available codes are actually used, deviating from their initial purpose to design cross-sections under eccentric axial compression actions, against the advice given by the same codes. For instance, the ACI 440-guide [9] does not recommend relying on FRP bars under compression, while the bars are especially experiencing such action under eccentric axial compression loading. Furthermore, the Canadian guideline [12] permits the use of FRP reinforcing bars in concrete under compression actions if their strength and modulus are ignored. Moreover, the FIB technical report [10] excludes only glass-FRP bars from use unless otherwise more experimental studies qualify the properties of FRP bars under such actions. Numerous studies (e.g., [13, 14]) have handled the limitations of such design guides and considered them conservative material. Recent studies have been conducted (e.g., [13, 15-17]) to demonstrate the feasibility of using FRP bars in RC elements subjected to axial compression forces. Such studies change the trend of some design guides to consider the contribution of FRP bars in concrete members subjected to compression forces. For instance, the recent version of the Canadian highway bridge design code [18] allows the use of FRP bars in FRP-RC columns subjected to eccentric force while considering their contribution until a compressive strain of 0.002 is reached.

Based on the recent trend towards using FRP bars under compression actions, it is important to provide the necessary safety factor(s) required for design purposes. Herein, the rules of ACI-318 [19] code format were considered to derive the ultimate axial eccentric capacity P_u of short concrete columns reinforced by means of steel bars. Nevertheless, the steel bars contribution is replaced by the FRP bars contribution. The ultimate capacity can be taken as $P_u=\phi(F_c+F_{FRP})$, where F_c and F_{FRP} are the internal forces carried by concrete and FRP bars, respectively. Evaluation of these forces depends mainly on the position of the neutral axis, strain profile across the RC section and concrete crushing strain ε_{cu}=0.003 (see Figure 1). ϕ is the strength reduction factor proposed to be calibrated in the present study. Currently, the ACI 440-1R-15 guide [9] proposes a strength reduction factor ϕ that addresses only FRP RC beams, as given in Eq. 1:

$$\phi = \begin{cases} 0.55 & \text{if } \rho_{FRP}/\rho_{FRP,b} \le 1.0 \\ 0.3 + 0.25\rho_{FRP}/\rho_{FRP,b} & \text{if } 1.0 < \rho_{FRP}/\rho_{FRP,b} < 1.4 \\ 0.65 & \text{if } \rho_{FRP}/\rho_{FRP,b} \ge 1.4 \end{cases} \quad \text{Eq. (1).}$$

where ρ_{FRP} and $\rho_{FRP,b}$ are the actual and balanced FRP reinforcement ratios, respectively.

$$\rho_{FRP} = \frac{A_{FRP}}{b.d} \quad \text{Eq. (2a)}$$

$$\rho_{FRP,b} = \frac{0.85\beta_1 f_c'}{f_{FRP,u}} \left(\frac{E_f \varepsilon_c'}{E_f \varepsilon_c' + f_{FRP,u}} \right)$$ Eq. (2b)

where *b* and *d* are the dimensions of the column section, A_{FRP} corresponds to the area if FRP bars, f_c' and $f_{FRP,u}$ are the concrete compressive and FRP tensile strengths, ε_c' is the extreme fibre concrete compressive strain in conjunction with f_c', E_f is the elastic modulus of FRP, and β_1 is the ratio between the depth of the equivalent rectangular concrete stress block and the neutral axis depth. Similar to steel-RC flexural members, two possible failure modes could occur. The first failure mode is tension failure mode (i.e., FRP rupture), which takes place when $\rho_{FRP} < \rho_{FRP,b}$. FRP rupture failure is a sudden and catastrophic mode. The compression failure mode (i.e., concrete crushing), which takes place when $\rho_{FRP} > \rho_{FRP,b}$, is marginally more desirable for flexural FRP-RC members. However, both FRP rupture and concrete crushing failure modes are acceptable in designing FRP-RC flexural members.

Existing codes of practice have fundamental structural safety uncertainties that have major implications for the structural design and safety of FRP RC elements. Inability to address this uncertainty issue may lead to uneconomic design in many situations. Updated design codes suggest that the value of the strength reduction factor ϕ should be evaluated using a mathematical calibration procedure that enables to consider the uncertainty inherited in design variables such as load, material, and geometry. The uncertainty of random variables should be treated using their statistical parameters, such as the mean value, standard deviation and probability density function. Calibration can be considered an optimization procedure that is used to achieve a certain goal over reliability classes of structures. This goal may be of safety, risk or economical type [20].

The reliability of concrete columns reinforced with conventional steel bars has been studied by several researchers. Frangopol *et al.* [21] performed a reliability analysis of steel-RC short/slender columns, in which the authors implemented Monte Carlo simulation to evaluate the reliability of steel-RC columns considering material nonlinearity. Structural responses were evaluated through a simplified buckling formula and sectional analysis. The results revealed that both the loading path and load correlation can affect the reliability of the columns. In another study by Diniz and Frangopol [22], the effect of long-term creep of concrete on the structural reliability of eccentrically loaded nonsway slender RC columns was investigated, where many design factors, such as the reinforcement ratio, load eccentricity and concrete strength (*i.e.,* normal and high strength concrete), were studied. The major conclusion drawn by the authors is that ACI-318 [19] code rules for the case of long steel-RC columns using high strength concrete are too conservative compared to the normal strength concrete case. The longitudinal reinforcement ratio showed a significant effect on the reliability of steel-RC columns with high eccentricities and high concrete strengths. Mirza [23] aimed to evaluate the strength reduction factor ϕ of tied slender steel-RC columns. The study recommended a strength

reduction factor with a value of 0.7 for the concrete crushing failure mode and linearly increased to 0.9 when the axial force dropped from a balanced value to zero.

Szerszen *et al.* [24] carried out a reliability-based calibration study. ACI-318 guide rules [19] were assumed, and their objective was to calculate the strength reduction factor for the design of different types of steel-RC members considering various load combinations in shear and flexural limit states. According to the authors, there is a need to decrease the strength factors in different situations of the ACI-318 rules. Such required decreases in strength factors should be followed by changes in load combination factors for dead and live loads. Although the study of Szerszen *et al.* [24] considers various loading combinations and structural types, the study relies on a limited number of design situations for each structural type or limit state. Moreover, from a reliability analysis point of view, the study does not provide a full probabilistic formulation of the problem, whereas it uses a simplified formula for calculating the reliability indices. Mohamed *et al.* [20] provided a reliability-based calibration procedure to obtain uniform reliability indices of steel-RC columns. The structural performance was obtained using a response surface method based on finite element simulations. Geometric and material nonlinearity were included in the finite element model. Partial safety factors were evaluated according to the Eurocode format. Many design parameters were considered in the analysis, such as the slenderness ratio, cross-section dimensions, reinforcement ratio, material strengths and load eccentricity. However, only the uncertainties in material properties (concrete strength and steel yield strength) were considered. Based on the results obtained, the proposed model provided a better format of steel and concrete safety factors, which results in a constant safety level. However, the safety factor format obtained was expressed in a very long polynomial relationship, which is not practical for design purposes. Putting the matter generally, reliability-based calibration of safety factors can show a certain level of inappropriateness of the design codes. As the initial approach of developing FRP-RC design guidelines was to modify conventional RC codes of practice, safety factors applied to FRP-RC members may be questionable.

A large number of research studies concerning the reliability-based design of FRP-strengthened reinforced concrete structural elements have been published in the recent literature. Most of these research studies deal with the use of FRP sheets or plates to strengthen RC beams (bridge girders) in bending [25-28], shear [29-31] or RC columns in compression [32,33]. Reliability-based approaches for the calibration of safety factors for FRP-bar RC members are very infrequent in the literature, mentioned mainly in the works of Behnam and Eamon [34] and Shahnewaz *et al*. [35]. The first article cited presents the reliability-based optimization of concrete flexural members reinforced with ductile FRP bars, but the authors insist mainly on the interest of using ductile vs brittle FRP bars and do not debate the calibration of the safety factor. In the second article cited, the authors dealt with the shear design equation for slender

concrete beams reinforced with FRP bars and stirrups using a genetic algorithm and reliability analysis. Nevertheless, the authors do not question the relevance of safety factors. Above all, these two articles do not deal with column members, which are the structural elements studied in the present work. At this point, it can be stated - considering the possible lack of relevancy, shown by many authors, of partial safety factors in current design guides or codes, and, that the case of short concrete columns reinforced with FRP bars has not yet been studied - that there is an interest to study the actual accuracy of the current design codes.

In summary, the main objective of this paper is to calibrate the strength reduction factor ϕ found in the ACI 440-1R15 design guide for short rectangular concrete columns reinforced with FRP bars. The ultimate eccentric axial force of the column will be obtained using sectional analysis (see section "2.1. Structural modelling"). The structural reliability will be presented in terms of reliability index β. First-order-reliability-method FORM-based quadratic response-surface RS was used to obtain the safety/reliability index for each case in the class of structure (see section "2.2. Structural Reliability aspects"). Loads, strength, and geometrical parameters are considered random variables. Statistical parameters (mean, standard deviation and distribution type) of all considered random variables are taken from previous studies available in the literature. The calibration approach is carried out in sequential steps (see section "3. Calibration procedure"). To ensure the applicability of these calibrated strength reduction factors to a wide range of situations, various configurations of short concrete column cases, for which experimental data are available, were considered. Generally, the reinforcement of concrete columns can be arranged in two different configurations. First, a uniform distribution of FRP bars around the four sides of the column is observed. Second, an unsymmetrical reinforcement configuration about the horizontal axis passes through the centre of gravity (*c.g.*), as shown in Figure 1. Secondary effects, such as long-term, environmental, local buckling of FRP bars, column slenderness and confinement effects due to transverse reinforcement, were neglected in the calculations. The results will be discussed in terms of the summation of squared differences between the target and the actual reliability for all structure classes considered (see section "4. Results and discussion").

2. Methods

2.1. Structural modelling

The present study focuses on short concrete columns reinforced with FRP bars under eccentric loading. In very simple terms, the design principle here relies on the simple condition that design capacity P_d is greater than or equal to ϕP_u (*i.e.,* $P_d \geq \phi P_u$), where P_u is the ultimate eccentric load of the column, and ϕ is the strength reduction factor, as mentioned before. In the case of columns under an axial load applied with high eccentricity, the section can be considered to work under both axial and bending forces. To determine the ultimate eccentric load P_u, a sectional

analysis procedure, also called the fibre section method, is conventionally used. The cross section of concrete columns reinforced with FRP bars was divided into several slices, as shown in Figure 1. Each slice simulates a fibre of the material running in the longitudinal direction of the RC member. The following two main assumptions were included in the fibre section method. First, the plane section remains planar before and after bending, *i.e.,* strain profile across the section is likely to be linear. Second, concrete and FRP bars are assumed to be perfectly bonded.

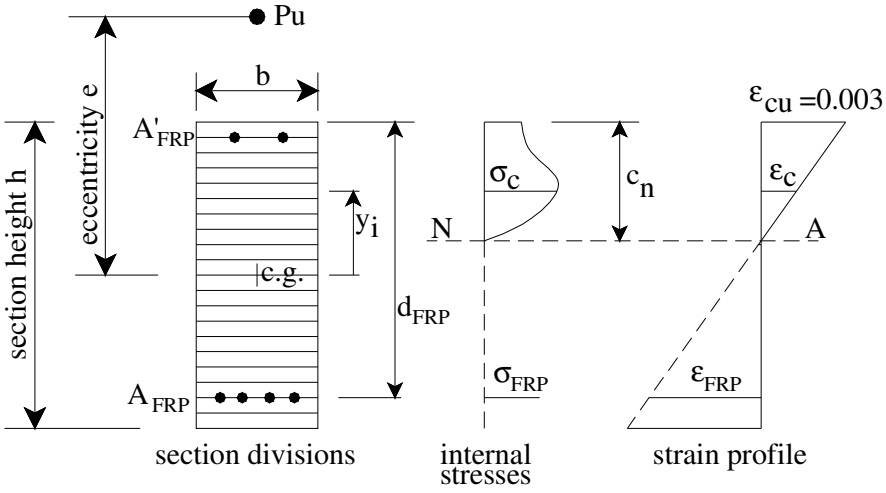

Figure 1. Discretization of concrete section.

Concrete compression is depicted by the following nonlinear stress-strain ($\sigma_c - \varepsilon_c$) law:

$$\sigma_c = f_c' \left(\frac{2\varepsilon_c}{\varepsilon_o} - \left(\frac{\varepsilon_c}{\varepsilon_o} \right)^2 \right) \quad \text{Eq. (3).}$$

where $\varepsilon_0 = 2f_c'/E_c$, E_c is the elastic modulus of concrete and was taken to be equal to $4700\sqrt{f_c}$ in MPa, adopted according to ACI 318-14 [19].

The tensile strength of concrete was assumed to be neglected. The stress-strain response of the FRP bars is assumed to be elastic-perfectly brittle; thus, the FRP stress can be evaluated as $\sigma_{FRP}=\varepsilon_{FRP}*E_{FRP}$, where ε_{FRP} and E_{FRP} are the strain in the FRP bar and elastic modulus of the FRP material, respectively. Nevertheless, FRP bars under compression strains are considered to have a modulus and strength lower than the modulus and strength for FRP bars under tensile strains, as stated in the ACI 440-1R-15 design guide [9] and as explained in §3. As mentioned above, two possible failure modes were considered. The first failure mode is concrete crushing, which takes place as compression strain in the upper fibre of the section reaches ε'_c, as shown in Figure 1. The second failure mode is FRP rupture, which takes place when the tensioned FRP reaches a strain equal to $f_{u,FRP}/E_{FRP}$ [36].

The following steps describe the procedure to obtain the ultimate eccentric force P_u:

1. Define column parameters such as eccentricity value *e,* material ($f_c^{'}$, ε_c', $f_{u,FRP}$, E_{FRP}) and geometrical properties (*b*, *h*, *A'FRP*, *AFRP*), and a tolerance ϵ for the calculation stop condition.
2. Specify the failure mode of either concrete crushing or FRP rupture.
3. Specify an initial position of the neutral axis c_n (which can be negative).
4. Calculate the strains in all concrete divisions and FRP bars and their corresponding stresses.
5. Thus, construct the following governing nonlinear function *f:*

$$f = e\ P_u - M_u = e\ \sum_{k=1}^{n} \sigma_k A_k - \sum_{k=1}^{n} \sigma_k A_k y_k \qquad \text{Eq. (4).}$$

   where σ_k is the stress applied on a specific area A_k (either concrete slice or FRP bar) whose centre is located at distance y_k from the centre of gravity of the column cross-section. M_u is the Bending moment.
6. The Newton-Raphson algorithm was used to update the unknown value of c_n involved in Eq. 4.
7. Repeat steps 4 to 6 until convergence is achieved (i.e., absolute value of function $f < \epsilon$), and the final value of c_n is obtained.
8. Check whether the specified failure mode, in step 2, is correct. Otherwise, repeat the analysis with the other failure mode.
9. Calculate the final ultimate load P_u according to Eq. 5:

$$P_u = \sum_{k=1}^{n} \sigma_k A_k \qquad \text{Eq. (5).}$$

The relevance of such a mechanical model is a crucial factor to be used for reliability analysis and should be checked by comparison with actual results. Thus, the accuracy of the sectional analysis algorithm in determining the eccentric ultimate capacity P_u has been verified using an experimental data set of seven specimens collected from [13, 37]. All specimens were concrete columns reinforced with FRP bars. Table 1 presents the geometrical and material properties of the collected specimens. The final column of the table provides the ratio (λ) between the experimental eccentric ultimate load $P_{u,exp}$ and theoretical ultimate load $P_{u,th}$. According to the statistics (mean and standard deviation) of the ratio λ, it can be concluded that the theoretical model used can accurately predict the ultimate eccentric load of concrete columns reinforced with FRP bars. This ability to predict the ultimate eccentric load of concrete columns reinforced with FRP was also confirmed in other previous studies (*e.g.,* [21, 38]), whereas the required ultimate load was found to be accurately predicted.

Calibration is performed over wide ranges of structural classes that are extracted from full combinations between ranges of eight design parameters including geometrical, material and loading characteristics: longitudinal FRP actual reinforcement ratio ρ_{FRP}, load eccentricity distance to column height ratio *e*/*h*, concrete compressive strength *f'c*, live load *LL* to dead load ratio *DL*, column height *h* to width *b* ratio (called also aspect ratio, *R*=*h*/*b*), amount of FRP in

compression zone to FRP in tensile zone ratio α, failure mode (concrete crushing or FRP rupture) and FRP grade (FRP tensile strength $f_{u,FRP}$ and FRP modulus E_{FRP}).

specimen	b (mm)	h (mm)	*cover* (mm)	e (mm)	f_c (MPa)	No of bars	bar size (mm)	f_{FRP} (MPa)	E_{FRP} (GPa)	$P_{u,exp}$ (kN)	$P_{u,th}$ (kN)	$\gamma_m = \frac{P_{u,exp}}{P_{u,th}}$
R-e10 [13]	150	150	20	15	35	6	16	629	38.7	693	645	1.07
R-e20 [13]	150	150	20	30	35	6	16	629	38.7	578	491	1.17
R-e30 [13]	150	150	20	45	35	6	16	629	38.7	354	366	0.97
Ge80 [37]	400	400	35	80	71	6	19	1236	62.7	5100	5182	0.98
Ge120 [37]	400	400	35	120	71	6	19	1236	62.7	3621	3569	1.02
Ge160 [37]	400	400	35	160	71	6	19	1236	62.7	2457	2356	1.04
Ge240 [37]	400	400	35	240	71	6	19	1236	62.7	1367	1301	1.05
											mean value of γ_m:	1.04
											standard deviation of γ_m:	0.07

$P_{u,exp}$ and $P_{u,th}$ are the experimental and theoretical eccentric ultimate loads, respectively.

Table 1: Geometrical and material properties of the experimental data set.

2.2. Structural Reliability aspects

The ultimate capacity of concrete columns reinforced with FRP bars can be presented in terms of the ultimate limit state G as follows:

$$G(X) = \gamma_m R - S = \gamma_m P_u(x_1, x_2, \dots x_n) - (P_{DL} + P_{LL}) \quad \text{Eq. (6).}$$

where γ_m is the model error, which reflects the uncertainty in the numerical procedure described in the previous section. R is the strength of the column, which corresponds to the ultimate eccentric load P_u. Such a load is a function of a vector of strength random variables $x=\{x_1, x_2 \dots x_N\}^T$, where the components x_i correspond to strength design parameters such as b, h, $f_{u,FRP}$,… S is the applied eccentric axial forces, including dead load P_{DL} and live load P_{LL}.

Structural reliability is expressed in terms of reliability index β, which is to be estimated in the standard Gaussian space [39] and is directly related to failure probability P_f (probability that function $G(x)$ is negative), through relationship $P_f = \Phi(-\beta)$, where Φ is the standard normal distribution. Therefore, the limit state $G(x)$, expressed in the physical space, must be represented in the standard Gaussian space $H(u)$. u represents a vector of standard normal variables $\{u_1, u_2, u_3 \dots u_n\}^T$ that corresponds to the x-vector. Principles of isoprobabilistic transformation T were used to obtain the function between x and u so that $u=T(x) \rightarrow H(u)=G(T^{-1}(u))$. The first order reliability method (FORM) was used to evaluate the reliability index β, which can be evaluated by solving the following constrained minimization problem:

$$\beta = \text{minimize} \sqrt{\sum_{i=1}^{n} u_i^2} \text{ under the constraint } H(U) \leq \text{zero} \quad \text{Eq. (7).}$$

The minimization problem given in Eq. 7 can be solved in an iterative procedure using the Hasofer–Lind–Rackwitz–Fiessler (HL–RF) procedure described in [39]. In this context, within the calculations of the FORM algorithm, the gradients of the limit state function $\{\nabla H(u_i)\}$ can be determined and normalized with respect to its norm $||\nabla H(u)||$, resulting in the sensitivity factor α_i of the reliability index with respect to the variable i:

$$\{\alpha_i\} = \left\{\frac{\partial \beta}{\partial u_i}\right\} = \frac{\{\nabla H(u^*)\}}{\|\nabla H(u)\|} \quad \text{Eq. (8).}$$

where u^* is a vector of random variables presented in the standard normal space at the most likely design point. Although the FROM method provides a full analytical solution of the problem, the FROM method approximates the actual limit state relationship given by Eq. 6 by a linear relationship at u^* [39]. Such an approximation needs to be verified via another trusted reliability method, as will be presented later.

For a certain random variable, the sensitivity factor α_i has two main advantages. First, α_i shows the contribution of its corresponding random variable to the reliability index. Second, the sensitivity factor sign of the variable under consideration reflects whether that variable positively or negatively affects the safety of the structure. Due to the high nonlinearity in the structural modelling, it was found to be difficult to express, directly, the required partial derivatives of the limit state function $H(u)$ with respect to each random variable u_i. Furthermore, numerical differentiation leads to a potential oscillation of the numerical procedures in the vicinity of the most likely design point [40]. Thus, full analytical forms of the derivatives of the function $H(u)$ are essential requirements. Therefore, the limit state $H(u)$ was approximated using the quadratic response surface RS, which can be expressed as:

$$H(u) = \theta_o + \sum_{i=1}^{n} \theta_i u_i + \sum_{i=1}^{n} \theta_{ii} u_i^2 = U\theta^T \quad \text{Eq. (9).}$$

where θ is the unknown coefficient vector, $\theta = [\theta_o\ \theta_1,\ \theta_2\ \dots\ \theta_n,\ \theta_{11},\ \theta_{22},\ \dots\ \theta_{nn}]^{\mathrm{T}}$, n is the number of variables and U is vector of basis polynomial functions $U = [1,\ u_1,\ u_2..u_n,\ u_1^2, u_2^2, u_i^2\ \dots\ u_n^2]^{\mathrm{T}}$. To obtain the coefficient vector θ, a dataset consisting of m=2n+1 u-vectors is constructed around a reference point u^* and their corresponding U m-vectors. The constructed dataset consists of two samples on each axis of the random variables ($u_i = u_i^* \pm r$, where r is an arbitrary scalar [41]). Accordingly, the vector of ultimate loads is obtained using the structural model described in the previous section. Defining a matrix V as $[U_1,\ U_2 \dots\ U_m]^{T}$, the vector θ can be calculated on the basis of minimizing the error between exact and approximated values in the constructed dataset. The conventional least squares method (*LS*) can be used to minimize such errors [42, 43], and the moving least squares MLS method can be used to provide a better approximation of the response function $H(U)$. MLS is a weighted LS method that involves weight functions $W(U)$ that depend on the approximation position. The MLS can be expressed as:

$$MLS = \sum_{j=1}^{m} \left(H\left({}_j u_1,\ {}_j u_2,\ {}_j u_i \dots {}_j u_n\right) - \theta_o - \sum_{i=1}^{n} \theta_i\, {}_j u_i - \sum_{i=1}^{n} \theta_{ii}\, {}_j u_{ii}^2 \right)^2 = (H(U) - U\theta)^T W(U)(H(U) - U\theta) \quad \text{Eq. (10).}$$

Hence, the estimate of θ can be expressed as

$$\theta = [V^T V]^{-1} W(U)[V^T H(V)] \quad \text{Eq. (11).}$$

where $W(U)$ is a diagonal matrix and can be defined as

$$W(U) = \begin{bmatrix} w_1 & 0 & \dots & 0 \\ 0 & w_j & \dots & 0 \\ \vdots & \vdots & \ddots & \vdots \\ 0 & 0 & \dots & w_m \end{bmatrix} \quad \text{Eq. (12).}$$

where w_j is the product of two weight functions and can be defined as follows [42]:

$$w_j = exp\left(-\frac{H(U_j)-H(U^*)}{H(U_j)}\right).exp\left(-\frac{D_j^2}{2}\right) \quad \text{Eq. (13).}$$

where $H(U_j)$ and $H(U^*)$ are the limit state functions at the j^{th} point ${}_ju$ and reference point u^*, respectively. D_j is the distance between the j^{th} point ${}_ju$ and reference point u^*. Eventually, the required response $H(U)$ or its derivatives with respect to a certain random variable $\partial H/\partial u_i$ can be obtained easily in a full analytical form given in Eq. 9. Herein, the most likely design point defined in the FORM algorithm was considered the reference point. Figure 2 shows the flow chart of FORM based on RS.

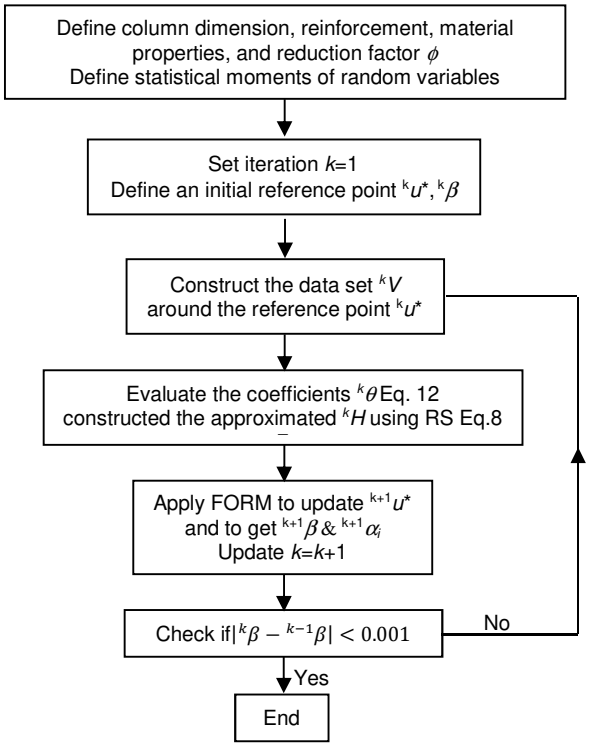

Figure 2. Summarized flow chart of FORM based on RS procedure.

Two main approximations are inherited in FORM-RS. First, the FORM algorithm is an approximate estimate of the reliability index and should be controlled with a simulation technique. Second, the RS method is an approximation of the ultimate limit state function *H(u)*. Therefore, FORM-RS should be verified using the structural reliability simulation method. From the other point of view, the use of crude Monte Carlo (MC) simulation is highly time consuming, especially in the case of a high number of random variables. Based on knowledge of the design point u^*, obtained using FORM-RS, a Monte Carlo-based importance sampling (MC-IS) simulation technique was used to validate the results of FORM-RS. To eliminate the approximation inherent in the RS method, the required structural responses for

the MC-IS technique were obtained directly using the structural model described in the previous section. *ns*-vectors of *u* are generated in the standard Gaussian space. Accordingly, the corresponding limit state function *H*(*u*) is evaluated based on the exact structural response given in the previous section. Hence, the estimate of the probability of failure can be expressed as:

$$p_f = \frac{1}{ns}\sum_{i=1}^{ns} I_f \, exp\left(-u^{*T}u_i - \frac{\beta^2}{2}\right) \quad \text{Eq. (14).}$$

where I_f is indicator failure (I_f=1 if H(u)<0, otherwise I_f=0). β is the reliability index obtained using FORM-RS.

3. Calibration procedure:

Concerning the design of FRP-reinforced concrete members under a pure bending moment, ACI-440 [9] provides the strength reduction factor ϕ given in Eq. 1 as a function of the FRP reinforcement ratio ρ_{FRP}. Thus, the main scope of the present study is to optimize the strength reduction factor ϕ given in Eq. 1 and to assess its variation with respect to various design parameters. The general design form of ACI [9, 19] codes for reinforced concrete members can be expressed as a combination of actions as given in the following equation:

$$\phi P_u = \gamma_G P_{DL} - \gamma_Q P_{LL} \quad \text{Eq. (15).}$$

where γ_G and γ_Q are dead and live load partial safety factors, which were taken to be equal to 1.2 and 1.6, respectively. P_u is the ultimate eccentric load obtained using Eq. 4-5. P_{DL} and P_{LL} are the applied eccentric dead and live loads, respectively.

As already mentioned, to ensure the generalization of these calibrated strength reduction factors to a wide range of situations, different combinations of design parameters (load eccentricity, aspect ratio of the concrete section, reinforcement ratio, live to dead load ratio, strength of concrete, grade of FRP bars) were considered. Two main reinforcement FRP configurations were considered. The first is the Top-Bottom configuration, where the FRP main reinforcement is located at the tensioned side with area $A_{FRP,k}$, while a secondary FRP reinforcement is located at the compressed side with area $A'_{FRP,k}$, (or expressed as a ratio $\alpha = A'_{FRP,k}/A_{FRP,k}$), as shown in Figure 3a. This configuration is more convenient for columns with high eccentric loads. The second configuration is the uniform configuration with FRP reinforcement uniformly distributed around the perimeter of the concrete section, which is more suitable for columns with small eccentric loads, as shown in Figure 3b.

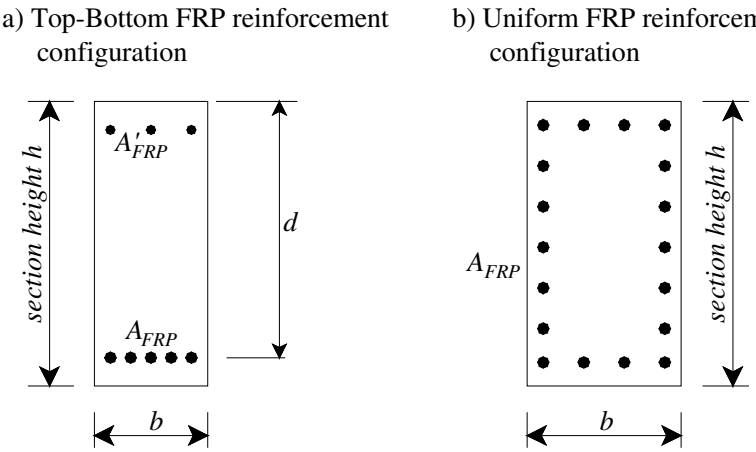

Figure 3. Top-Bottom and Uniform FRP reinforcement configuration.

Table 2 presents the range of the characteristic values of each design parameter. According to this table, the total possible number of combinations is 64800 and 34560 classes of structures for the Top-Bottom and Uniform FRP reinforcement configurations, respectively. The maximum spacing between longitudinal FRP bars in the case of the uniform configuration is taken to be equal to 150 mm, as recommended by ACI-318 [19], while the effect of side bars in the Top-Bottom configuration required to resist secondary effects (e.g., shrinkage of concrete) is neglected in the calculation of the ultimate eccentric load. Referring to Table 2, $\rho_{FRP}/\rho_{FRP,b}$ values are chosen such that they cover all the possible categories provided by Eq. 1 proposed by the ACI-440 committee [9]. Nevertheless, $\rho_{FRP,b}$ is evaluated so that it is related not only to material properties as for FRP RC beams (see Eq. 3b) but also, it is related to loading properties.

Parameter	Values (units)
Column width b_k	200, 350 and 500 (mm)
FRP reinforcement ratio $\rho_{FRP}=A_{FRP,k}/b_k d_k$	0.5, 1, 1.5, 2 and 2.5 times $\rho_{FRP,b}$ for Top-Bottom configuration. Ranges from 0.01 to 0.08 with an increment 0.01 for Uniform configuration.
Concrete compressive strength f'_{ck}	20, 30, 40, 50 and 60 (MPa)
Cross section aspect ratio $R=h_k/b_k$	1, 2, 3 and 4.
Eccentricity ratio e/h_k	0.1, 0.3, 0.5, 0.7, 1 and 1.5 for Top-Bottom configuration. 0.05, 0.1, 0.15, 0.2, 0.25 and 0.3 for uniform configuration
FRP Compression renforcement ratio $\alpha=A'_{FRP,k}/A_{FRP,k}$	0.2, 0.6 and 1 applied only in case of Top-Bottom, configuration
FRP ultimate strength $f_{FRP,k}$	500, 1200 and 2000 for FRP grades I, II & III, respectively (MPa)
FRP modulus of elasticity $E_{FRP,k}$	35, 70, 120 for FRP grades I, II & III, respectively (GPa)
Live load to Dead load ratio $P_{LL,k}/P_{DL,k}$	0.5, 1.5, 2.5 and 4.0

The subscript k refers to the characteristic value of the variables. $d_k=h_k$-c. where c (=25 mm) is the concrete cover. The properties of FRP grades I, II and III approximately represent the typical properties of glass, aramid and carbon of FRP bars, respectively, considered in the ACI-440 guide.

Table 2: Values of characteristic design parameters.

ACI-440.1R-15 [9], FIB [10], and ISIS Canada [11] stated, based on experimental studies, that the strength and modulus of FRP bars under compression are lower than the strength and modulus of FRP bars under tension actions. ACI-440 reduces the compressive strength and compression modulus of FRP bars depending on their type: glass

(GFRP) or carbon (CFRP) bars. ACI 440 reports that the compressive strength of FRP bars is approximately 55 and 78% of their tensile strength for GFRP and CFRP bars, respectively. Additionally, ACI-440 recommends compression moduli of 80 and 85% of the tensile modulus for GFRP and CFRP bars, respectively. The FIB guide [10] accredits the same recommendations for the compression modulus of FRP bars. Nevertheless, ISIS [11] considers that the compression modulus ranges between 77 and 97% of the tensile modulus. In addition, ISIS proposes that the tensile strength of FRP bars is strongly related to the fibre-volume ratio. In a recent experimental study, Khorramian and Sadeghian [44] demonstrated the importance of performing compression tests to estimate the compression strength rather than relating the compression strength to its tensile strength due to the wide variation in the FRP bar compressive strength. The study proposes a compressive strength almost equal to the tensile modulus for GFRP bars. Herein, as ACI-440 is the matter of the study, it is proposed to follow all ACI-440 recommendations for the mechanical properties of FRP bars under compression. Therefore, compressive strength and compression modulus were adopted using reductions of 0.55 and 0.8, respectively, of their corresponding tensile properties for both GFRP and CFRP bars. The choice of the reduction factor (=0.8) that concerns the compression modulus is based on the reported range being small (e.g., ≈0.8→0.85 [9]). Hence, for more conservatism, a lower value is considered. Concerning the compressive strength, the FRP ultimate compressive strain was specified as 0.55*500/(0.8*35000)=0.01, 0.55*1200/(0.8*70000)=0.012, and 0.55*2000/(0.8*120000)=0.011 for grades I, II and III, respectively, as reported in Table 2. The ultimate compressive strain cannot be reached, as their values are greater than three times the ultimate concrete compressive strain (=0.003).

The calibration procedure considers the randomness of the mechanical model error, loads, geometrical and material properties. Table 3 presents the statistical parameters (mean, standard deviation, distribution type) of the random variables considered in the reliability analyses.

Variable	Distribution	Units	Characteristic	Mean (*Bias*[a])	Std[b] (*CoV*[c])	Source
$f_{FRP,}$	Weibull	MPa	See Table 2	(1+3**CoV*)	(0.05)	[45], [9]
E_{FRP}	Normal	GPa	See Table 2	(1)	(0.05)	[45]
A_{FRP}	Normal	mm^2	$A_{FRP,k}$	(0.97)	(0.015)	[45]
f'_c	Log-normal	MPa	See Table 2	$\max\begin{cases}\frac{f'_{ck}}{1-1.34CoV}\\ \frac{(f'_{ck}-3.5}{1-2.33CoV}\end{cases}$; if f_{ck}<=35 $\max\begin{cases}\frac{f'_{ck}}{1-1.34CoV}\\ \frac{0.9f'_{ck}}{1-2.33CoV}\end{cases}$;if f_{ck}>35	(0.16)	[22,19]
b	Normal	mm	b_k	b_k+1.5	6.35	[22]
h	Normal	mm	h_k	h_k+1.5	6.35	[22]
Dead load P_{DL}	Normal	kN	$P_{DL,n}$	(1.05)	(0.1)	[20-22]
Live load P_{LL}	Extreme type I	kN	$P_{LL,n}$	(1)	(0.25)	[22]
Model error γ_m	Normal	---	1	1	0.025+0.18e/h_k≤0.11	[23]

[a]Bias; Mean value/nominal value, [b]Std standard deviation, [c]*CoV*; coefficient of variation.

Table 3: Probabilistic parameters of random variables.

The calibration procedure aims to determine the value of the strength reduction factor ϕ that minimizes the function:

$$f(\phi, \beta_T) = \sum_{i=1}^{N} \omega_i (\beta_i - \beta_T)^2 \quad \text{Eq. (16).}$$

over the *N* classes of structures considered [25, 46] and where β_T is the target reliability index considered in codes. β_i, w_i are reliability index and weight/frequency of a certain class of structure (*i*) of the considered class of structures. The corresponding frequency ω_i for each i^{th} class of structure means that $\sum_{i=1}^{N} \omega_i$=unity. Herein, all design situations were assumed to have an equal frequency of 1/*N*, where *N* is the number of situations in the combination set. All mathematical calculations were carried out using MATLAB software [47]. To perform the calibration algorithm, the following introductory data should be defined: *N*-class of structures (depending on the expected ranges of design variables), failure modes, design rules (Eq. 15), goal of the code, the target reliability index β_T (*i.e.,* according to Szerszen and Nowak [24], ACI-318 code β_T proposes a target reliability index β_T of a value equal to 4.0 for the design of RC columns), and set of size *M* of strength reduction factors (i.e., ϕ=0.5:0.025:0.9). Consequently, the calibration procedure was performed according to the following main steps [25]:

1. Initiate counter *j,* which represents the strength reduction factor under consideration.
2. Select a j^{th} ϕ_j of the *M* values of the strength reduction factor set.
3. Initiate counter *i,* which represents the class of structures under consideration.
4. Choose an i^{th} case of the *N* class of structures (*i.e.,* a set of $[b_k, r_{FRP}, f'_{ck}, R, e/h_k, \alpha, f_{FRP,k}, E_{FRP,k}, P_{LL}/P_{DL}]^i$ according to Table 2). Then, provide the corresponding frequency ω_i for each i^{th} class of structure such that $\sum_{i=1}^{N} \omega_i$=unity. Herein, all design situations were assumed to have an equal frequency of 1/*N*, where *N* is the number of situations in the combination set.
5. Deduce from this set the value of P_u using the structural model described by Eq. 4 and Eq. 5. Then, calculate the applied working loads P_{LL} or P_{DL} from Eq. 15.
6. Apply FORM-RS algorithm to Eq. 6 to calculate the reliability index β_i considering probability laws presented in Table 3. The results of FORM-RS can be verified using the MC-IS procedure using Eq. 14.
7. Update the value *i* (i.e., *i*=*i*+1), then repeat steps 4 to 6 until counter *i* reaches *N.*
8. Evaluate the penalty function $f_j(\phi_j)$ using the least square form given in Eq. 16.
9. Update the value *j* (i.e., *j*=*j*+1), then repeat steps 2 to 8 until counter *j* reaches *M.*
10. Choose the optimum value of ϕ that corresponds to the minimum penalty functions.

The calibration outlined above is the most widely used calibration algorithm and has been described in many previous studies, such as [25, 46]. Although the procedure can be applied in a simple manner and does not require a complicated optimization method, the procedure needs a huge number of calculations (*i.e.,* calculations are to be performed for all classes of structures and repeated at each value of ϕ in the assumed range).

Referring to the previous section, FORM-RS has two main approximations: the first is the linear approximation of the limit state function, while the second is the use of the response surface approximation. To determine the accuracy results obtained via the FORM-RS method, structural reliability results obtained using FORM-RS were verified with MC-IS using two samples of sizes equal to $ns=10^3$ and $ns=10^4$. Table 4 presents ten reliability results – as sample results - arbitrarily chosen cases that cover the extent of the design parameters. The last three columns of the table provide the reliability indices obtained using FORM-RS, MC-IS considering $ns=10^3$ and MC-IS considering $ns=10^4$. The proposed FORM-RS algorithm could predict the reliability index accurately, as its results are very close to the results obtained using the MC-IS technique. Differences between the FORM-RS and MC-IS methods do not exceed 2.5%, which reflects the accuracy of using both the FORM and RS methods regardless of the change in section configuration or the value of the design variable.

Sample	b_k mm	R	f_{ck} MPa	*FRP Grade*	e/h_k	$\frac{P_{LL,k}}{P_{DL,k}}$	Reinforcement		ϕ	Reliability index β			% Error
							configuration	FRP amounts		FORM-RS	MC-IS $ns=10^3$	MC-IS $ns=10^4$	
1	200	2	40	I	1.5	0.5	Top-Bottom	$\rho_{FRP}=1.5\rho_{FRP,b}$ α=1.0	0.50	6.80	6.76	6.77	0.44
2	350	3	50	II	0.3	1.5	Top-Bottom	$\rho_{FRP}=2.5\rho_{FRP,b}$ α=0.2	0.55	4.99	4.95	4.97	0.40
3	500	4	60	III	1.5	2.5	Top-Bottom	$\rho_{FRP}=2.5\rho_{FRP,b}$ α=1.0	0.60	4.52	4.51	4.51	0.22
4	200	2	30	I	0.7	1.5	Top-Bottom	$\rho_{FRP}=2.5\rho_{FRP,b}$ α=0.2	0.65	4.48	4.50	4.46	0.45
5	350	1	20	II	0.5	0.5	Top-Bottom	$\rho_{FRP}=1.0\rho_{FRP,b}$ α=0.6	0.75	4.03	3.94	3.94	2.28
6	350	4	30	II	0.3	1.5	Uniform	$\rho_{FRP}=0.05$	0.50	5.28	5.23	5.26	0.38
7	500	1	20	III	0.1	0.5	Uniform	$\rho_{FRP}=0.08$	0.55	4.99	4.90	4.91	1.62
8	500	2	40	III	0.25	0.5	Uniform	$\rho_{FRP}=0.01$	0.60	5.09	5.00	5.01	1.60
9	200	3	40	I	0.25	2.5	Uniform	$\rho_{FRP}=0.04$	0.65	4.14	4.10	4.11	0.73
10	350	3	50	II	0.15	2.5	Uniform	$\rho_{FRP}=0.06$	0.75	3.80	3.80	3.76	1.06

where *ns* is the number of importance sampling simulations. % Error=100| $\beta_{\text{FORM-RS}}$- $\beta_{\text{MC-IS}}$ |/$\beta_{\text{MC-IS}}$

Table 4: Verification of FORM-RS results with MC-IS simulation.

4. Results and discussion

Generally, the value of the target reliability index β_T is specified by design codes depending on the consequences and costs of failure. For the flexural limit state, ACI-440 [9] recommends a target reliability index (β_T) ranging from 3.5 to 4, which was also previously proposed by Szerszen and Nowak [24] for designing flexural members under compression control. In the present study, β_T is considered equal to 4 to ensure a safer design. The reliability indices for all classes of structures were evaluated. Then, the penalty functions $f(\phi)$ were calculated and plotted in Figures 4 and 5 for the Top-Bottom and Uniform FRP reinforcement configurations, respectively. The idea of creating these figures is to observe and quantify the effect of certain design variables on the factor $\phi*$ that minimizes the function $f(\phi)$ given by Eq. 16. The curves shown in Figures 4 and 5 are characterized by a decrease in $f(\phi)$ as ϕ increases until $f(\phi)$ *reaches its*

minimum at ϕ^*; thereafter $f(\phi)$ increases again. Values of ϕ before ϕ^* correspond to $\beta>\beta_T$ resulting in underdesign, while values of ϕ after ϕ^* correspond to $\beta<\beta_T$ resulting in overdesign. Generally, underdesign is penalized/desirable more than overdesign. According to the figures, the optimum strength factors lie in the range ϕ=0.65→0.75, which is higher than the range given for flexural design provided by Eq. 1 (ϕ=0.55→0.65), due to the nature of failure in each problem. Moreover, β_T required for flexural design is equal to 3.5, which is lower than β_T required for column design [24]. In addition, the variations in P_{LL}/P_{DL} (in Figures 4e and 5f) and *e/h* (in Figures 4b and 5b) are observed to cause the most notable changes in the minimal value of the penalty function $f(\phi)$ and their corresponding reduction factors. For the Top-Bottom configuration, minima of the function $f(\phi)$ can be reached for $\phi*$ values ranging between 0.8→0.65 and 0.675→0.75 for P_{LL}/P_{DL} and *e/h* ranging between 0.5→4 and 0.1→1.5, respectively. Similarly, for the uniform configuration, minima of the function $f(\phi)$ can be reached for $\phi*$ values ranging between 0.75→0.65 and 0.65→0.7 for P_{LL}/P_{DL} and *e/h* ranging, respectively, between 0.5→4 and 0.05→0.3, respectively.

Accordingly, the FRP reinforcement Top-Bottom configuration requires a slightly higher reduction factor than the uniform configuration because the Top-Bottom configuration relies on the mode of failure, *i.e.,* the FRP rupture failure mode requires values of ϕ (=0.65) lower than the concrete crushing failure mode (=0.725), as shown in Figure 4g. Regarding the f_c parameter (in Figures 4d and 5c), a slight variation in factor ϕ can be observed in both considered configurations. In the same concern as all other design parameters, no significant change in ϕ can be noted as their penalty functions $f(\phi)$ reach their minimum values at a strength factor ϕ equal to 0.725 and 0.7 for the Top-Bottom and Uniform FRP reinforcement configurations, respectively.

Figures 4h and 5g involve global curves, named "*all cases*", which express the function $f(\phi)$ for all classes of structures regardless of the failure mode. $f(\phi)$ reaches the minimum values at $\phi*$ equals to 0.725 and 0.675 for the Top-Bottom and Uniform configurations, respectively. However, considering these values of $\phi*$ results in 65.2 and 53.8% of considered classes having $\beta<\beta_T$ (overdesign) for Top-Bottom and Uniform configurations, respectively. Thus, there is a need to consider a strength factor lower than the strength factors obtained from Figures 4 and 5, as presented in the later paragraphs.

Referring to the Top-Bottom FRP reinforcement configuration where either FRP rupture or concrete crushing failure modes can take place, it is important to quantify to what extent the ACI design rules agree with the concept of design points (u^*) in predicting the same failure mode. Hence, the relevance of ϕ to the failure mode is avoided. The inconsistency in the failure mode between the ACI design rules and the concept of the design point takes place due to changes in the material and/or geometrical properties in the two design procedures. Figure 6 shows the % class of

structures that failed by FRP rupture according to ACI rules and those failed by FRP rupture according to both ACI rules and the concept of the design point (u^*) obtained using the FORM-RS algorithm. A large gap between the two curves at a small reduction factor ϕ can be observed. This gap decreases as ϕ increases and totally vanishes at ϕ = 0.9. In addition, the number of situations that failed due to FRP rupture does not exceed 3.5% of the total number of situations (=64800), whereas the dominant failure mode in most design classes of structures is concrete crushing.

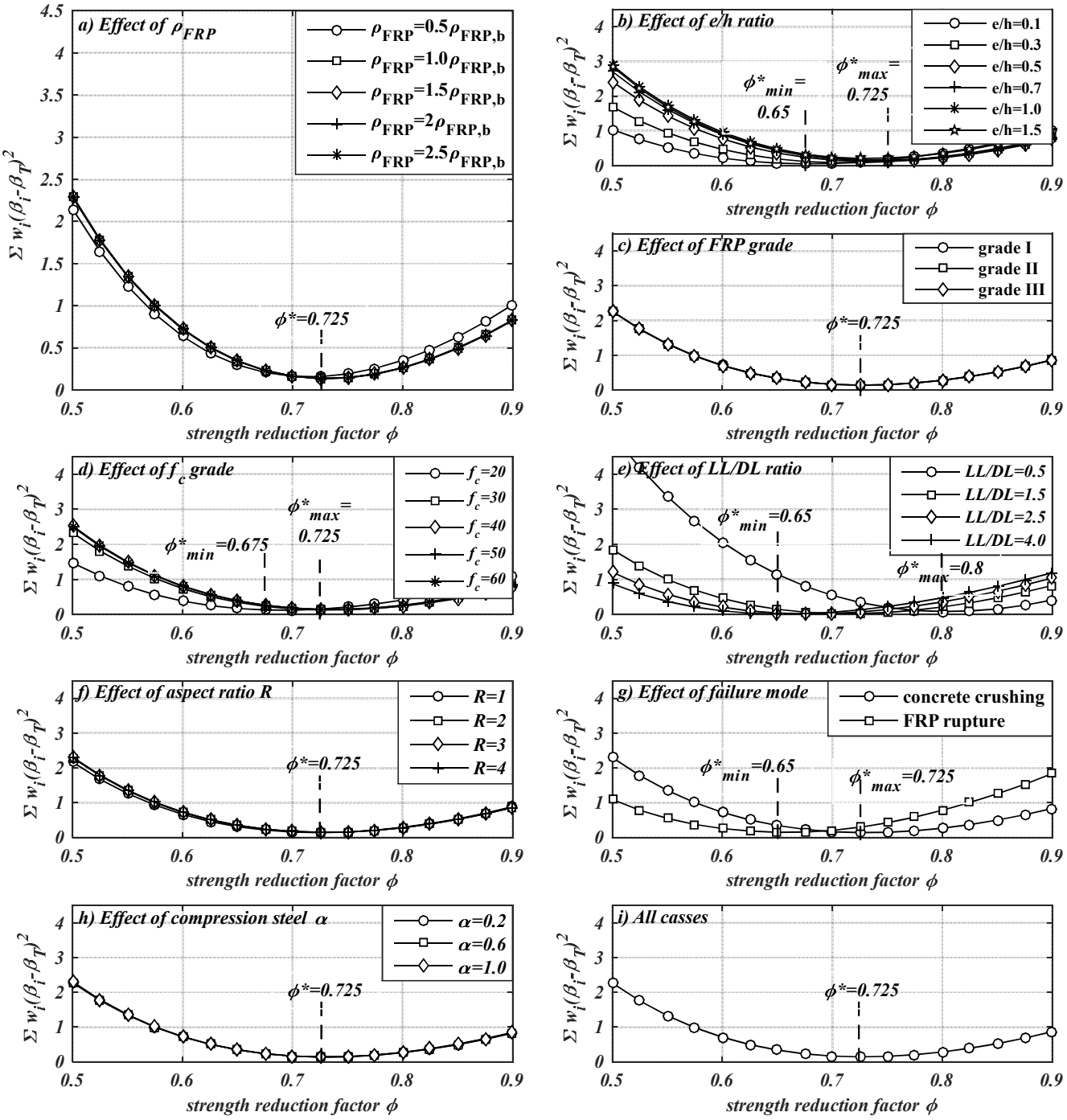

Figure 4: Evaluation of penalty function versus strength reduction factor ϕ (Top-Bottom configuration).

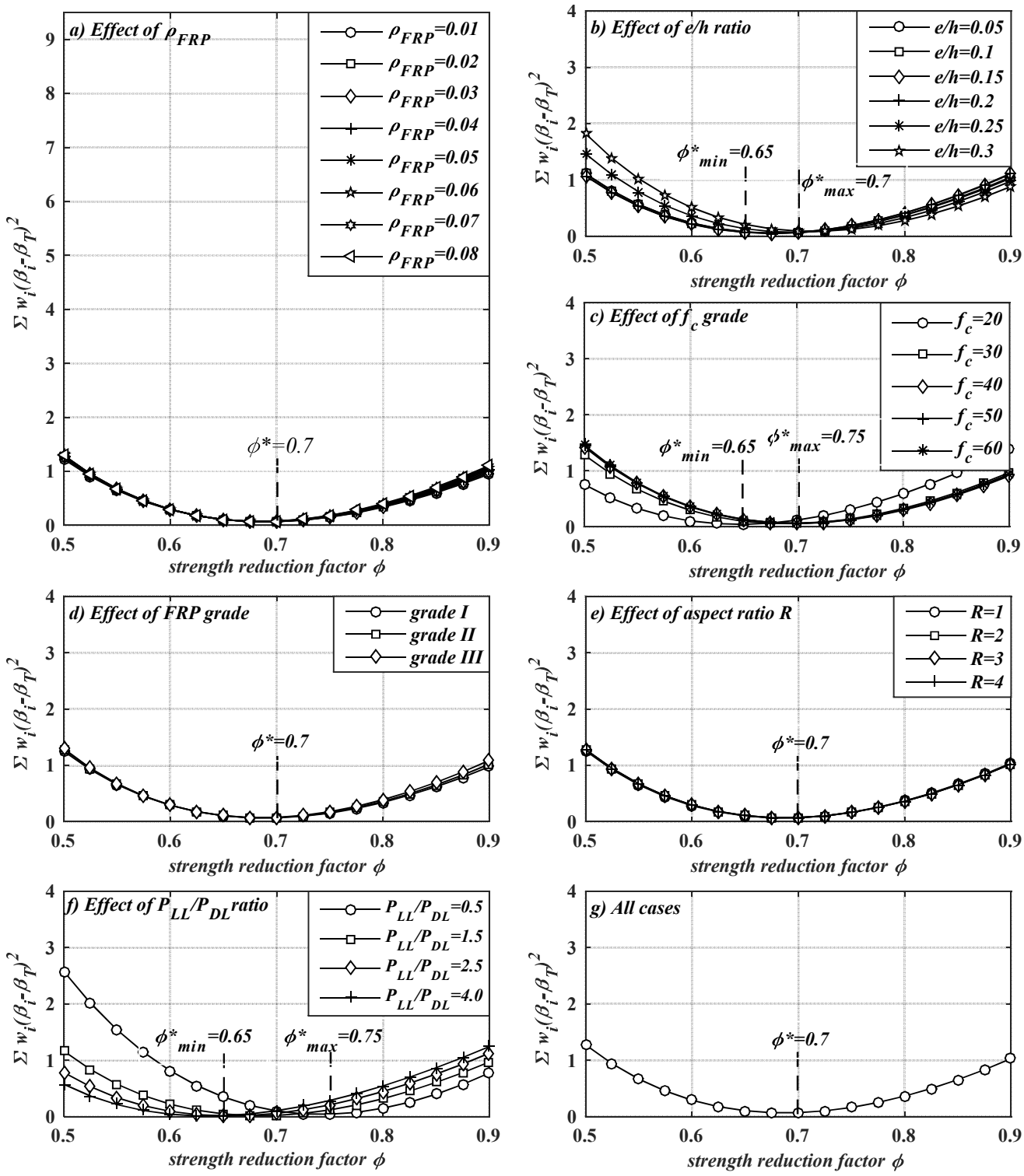

Figure 5: Evaluation of penalty function versus strength reduction factor ϕ (uniform configuration).

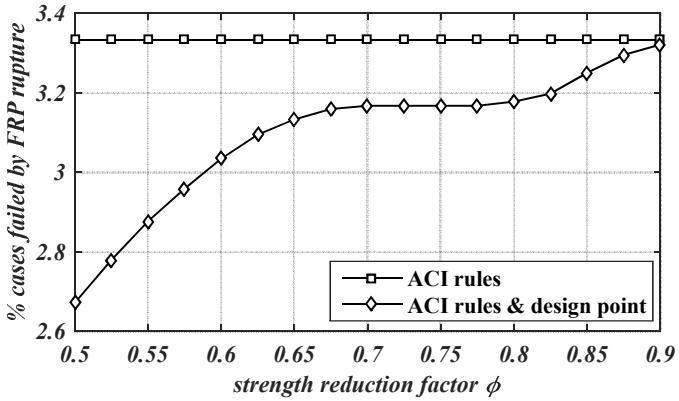

Figure 6. Class of structure number failed by FRP rupture (Top-Bottom reinforcement configuration).

The necessity to enhance the ACI approach is highlighted, and a way to estimate the strength reduction factor for FRP-reinforced RC columns is proposed. Providing a strength reduction factor ϕ to the designer is a quite difficult decision and requires more analyses of the data provided obtained using a calibration algorithm. The proposed calibration procedure enables the evaluation of the reliability index for all classes of structures at different strength factors. Minimum, maximum, and average values of reliability indices were recorded at each considered strength factor during the calibration procedure. Figures 7 and 8 show plots of these values versus their corresponding strength reduction factors ϕ for the Top-Bottom and Uniform FRP reinforcement configurations, respectively. Such plots could enable information about minimum (worst safety level) and maximum reliability index values that will be reached after design. According to the figures, a strength reduction factor of approximately ≈0.6 can be suggested for designers to provide a reliability index of $\beta \geq 4.0$. This suggested strength reduction value (ϕ=0.6) is close to the average value given by the ACI-440 rules in Eq. 1 regardless of the $\rho_{FRP}/\rho_{FRP,b}$ ratio, which is valid for pure flexural design, as reported in the ACI-440 guide [9]. Moreover, only 1403 (2,2%) and 1116 (3,2%) classes of structures are found to have a reliability index lower than β_T for the Top-Bottom and Uniform configurations, respectively, when ϕ=0.6. Nevertheless, if the global minima of the function *f* for all cases are considered, strength factors ϕ of 0.725 and 0.7 for Top-Bottom and Uniform cases, respectively, can be proposed, as shown in Figures 4i and 5g. For these values of reduction factors, 42308 (65.3%) and 25299 (73,2%) classes of structures are recorded to have reliability indices lower than β_T for the Top-Bottom and Uniform configurations, respectively. However, ϕ=0.6 could be recommended to maintain more than 95% of situations that match the requirements of the ACI code ($\beta \geq \beta_T$) for the design of RC columns.

Referring to the Top-Bottom configuration, FRP rupture and concrete crushing failure modes could possibly occur. Figures 7a and 7b show that concrete crushing provides higher reliability indices if the same strength reduction factor is considered because tension failure relies on the variation in both concrete and FRP materials, while compression

failure relies only on the variation in concrete material. This context matches the ACI-440 recommendation, as it considers the concrete crushing failure mode for FRP-RC members under flexural loading, which is marginally more desirable than FRP rupture. From this point of view, compression failure can be recommended for FRP-RC columns because it provides a more desirable and safer design than tension failure.

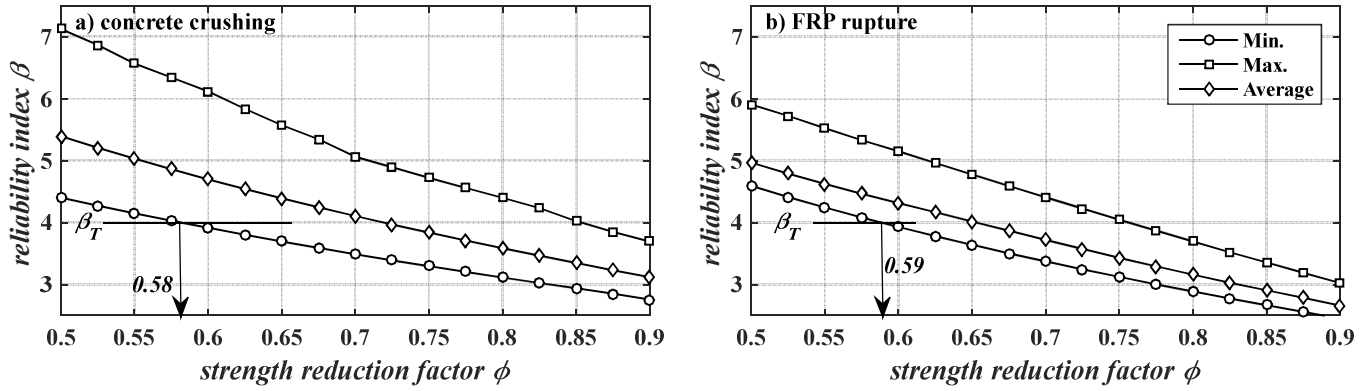

Figure 7. Minimum, average, and maximum reliability index recorded versus strength reduction factor ϕ (Top-Bottom configuration).

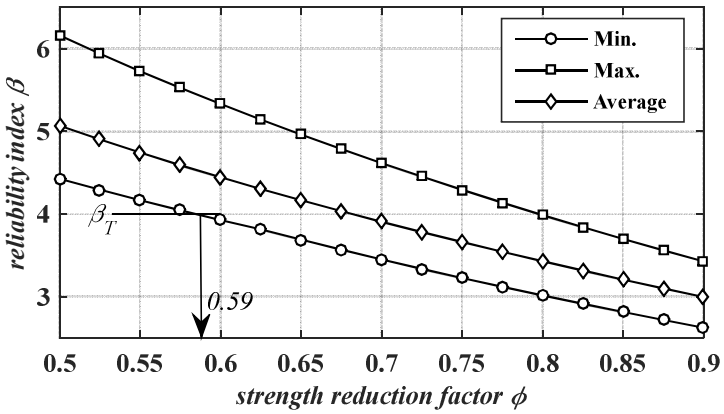

Figure 8. Minimum, average, and maximum reliability index recorded versus strength reduction factor ϕ (Uniform configuration).

The proposed calibration algorithm can be considered for any other target reliability index (β_T). However, Figures 7 and 8 simplify this step by choosing the target reliability index and evaluating the corresponding strength reduction factor (ϕ). Considering the minimum values of the reliability index in the figures could provide a conservative value of ϕ for design purposes and ensure a level of safety greater than the target value, *e.g.,* considering β_T=3.5. Thus, a strength factor of ϕ=0.69 is required for uniform configuration.

It is now obvious from the above discussion that using a fixed value of the strength reduction factor leads to uneconomic design [11]. As previously observed, (P_{LL}/P_{DL}) and (e/h) are the most important design parameters that could significantly affect the strength factor. Thus, proposing a strength factor related to these two design parameters

results in a more economic design than using a fixed value. Consequently, the penalty function *f* was evaluated with respect to each combination of each value of the P_{LL}/P_{DL} and *e/h* parameters reported in Table 2. The minimum values of $f(\phi)$ and their corresponding ϕ with respect to each combination of (P_{LL}/P_{DL}) and (*e/h*) were calculated. Thus, the values of ϕ were fitted against P_{LL}/P_{DL} and *e/h* in a quadratic response polynomial function. The fitted functions are as presented in Eq. 17a and 17b for the Top-Bottom and Uniform configurations, respectively,

$$\phi = 0.7941 - 0.1083\left(\frac{P_{LL}}{P_{DL}}\right) + 0.0152\left(\frac{P_{LL}}{P_{DL}}\right)^2 + 0.1614\left(\frac{e}{h}\right) - 0.0846\left(\frac{e}{h}\right)^2 \quad \text{Eq. (17a).}$$

$$\phi = 0.7701 - 0.068\left(\frac{P_{LL}}{P_{DL}}\right) + 0.2223\left(\frac{P_{LL}}{P_{DL}}\right)^2 + 0.0086\left(\frac{e}{h}\right) + 0.9821\left(\frac{e}{h}\right)^2 \quad \text{Eq. (17b).}$$

It is important to evaluate the levels of safety provided by these equations with respect to the reduction factor of a fixed value (*i.e.,* ϕ=0.6). Figure 9 shows a comparison, considering all 64800 and 34560 classes of structures for Top-Bottom and Uniform FRP reinforcement configurations, between the minimal/maximal values of reliability indices β calculated either with the strength factor ϕ values obtained using Eq. 17 or with a fixed value of ϕ equal to 0.6. In addition, Eq. 1, which follows the ACI-440 design guide for FRP RC beams, has been applied to the considered classes of structures. The effectiveness of the proposed values of ϕ can be achieved by decreasing the % number of cases having $\beta<\beta_T$ and decreasing the gap between the maximum recorded β indices to provide more economic design. According to Figure 9a (case of the Top-Bottom configuration), Eq. 17a significantly decreases the gap between the maximum and minimum recorded reliability indices. Therefore, a more economic design and more uniform reliability index are provided. In addition, the maximum reliability index approaches the target value β_T, which means that more economic design is achieved. However, 44% of structural classes tend to provide β lower than β_T, which illustrates that Eq. 17a may provide a more economic but less safe cross-section than using a fixed factor ϕ=0.6. Applying a 10% reduction of the values of ϕ given using Eq. 17a could improve the safety considerations since only 4.76% of structural classes will now have a β lower than β_T. Unlike the Top-Bottom configuration, the Uniform configuration (Figure 9b) with a fixed strength factor provides a safer and more economical cost than the cost given by Eq. 17b. Furthermore, Eq. 1 proposed by the ACI-440 guide results in safe but uneconomic design for the Top-Bottom configuration, as it provides higher values of safety levels (β). Moreover, the use of Eq. 1 in designing the uniform reinforcing configuration results in an unsafe design for more than 30% of cases. which can reflect the need for lower values of the strength reduction factor for design purposes for FRP-RC columns with Uniform configurations.

Finally, it can be recommended that a strength reduction factor ϕ taken at 90% of the varying values given by Eq. 17a should be used for optimal design for the Top-Bottom configuration. In contrast, a fixed value of ϕ at 0.6 could be used

for Uniform configurations.

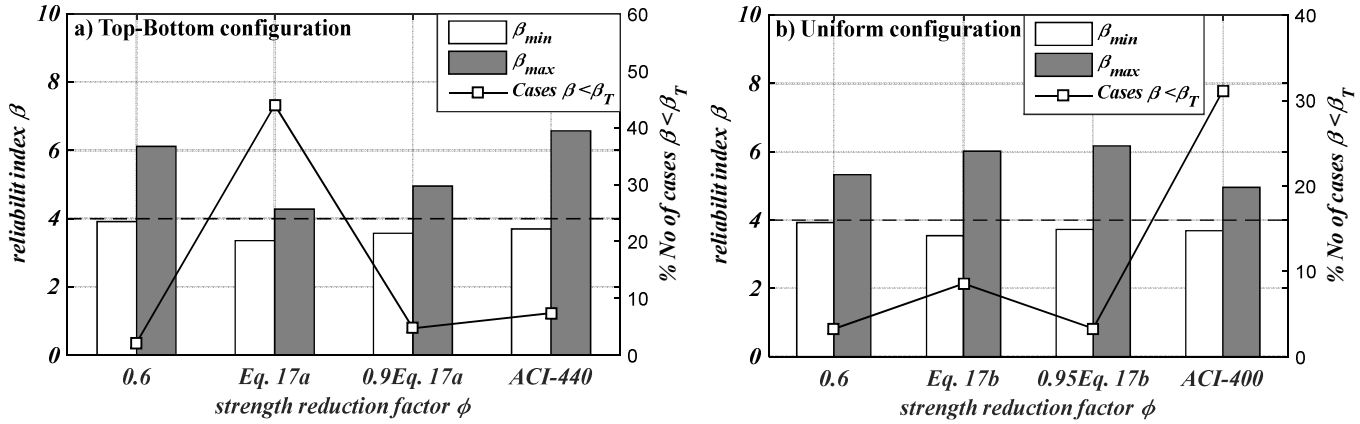

Figure 9. Assessment of varied versus fixed strength reduction factor.

Referring to the basic aspects of the structural reliability section described above, the first-order reliability method (FORM) can be used for sensitivity analysis (Eq. 8), which basically aims to differentiate between the considered random variables that could be treated as random or deterministic variables. Hence, the sensitivity analysis also aims to decrease the dimensions of the reliability problems to address. Figures 10 and 11 provide the range of sensitivity factor α_i for each random variable *i* considered within the reliability analysis for both reinforcement configurations. It can be emphasized that the concrete compressive strength f_c, section dimensions (*h* and *b*), model error γ_m, and loads are the variables of first importance and could significantly affect the results of the reliability analysis in both considered failure modes. The importance of the remaining variables depends on the failure mode of the columns; *e.g.,* the area of the FRP bars A_{FRP} and ultimate strength of the FRP bars f_{FRP} can be treated as deterministic variables when the concrete crushing failure mode occurs, while the column *b* width, concrete compressive strength f_c and modulus of the FRP bars E_{FRP} can be treated as deterministic variables when the rupture failure mode occurs.

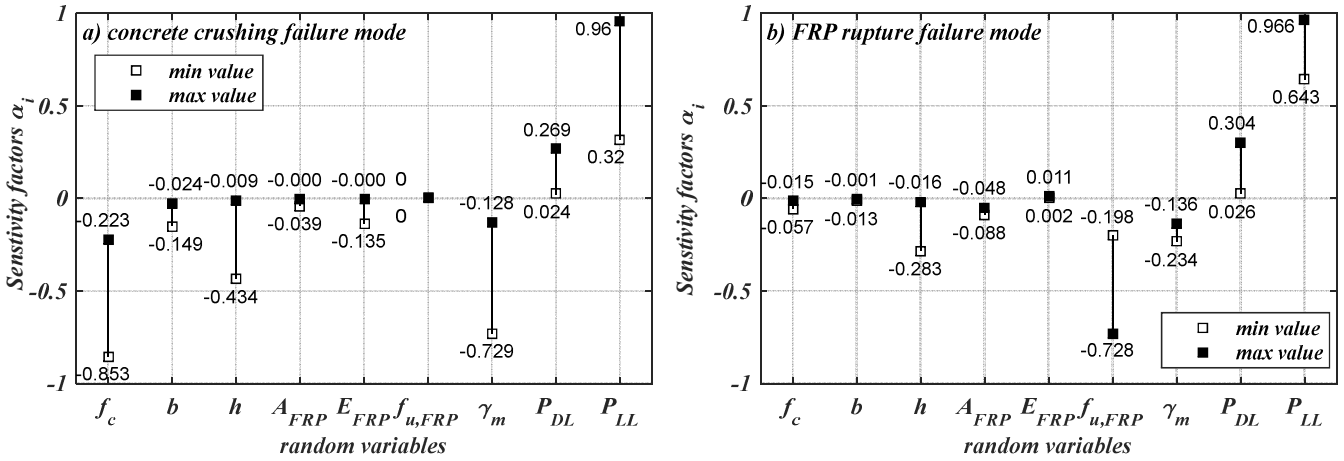

Figure 10. Maximum and minimum values of sensitivity factors α_i of random variables considered (Top-Bottom configuration).

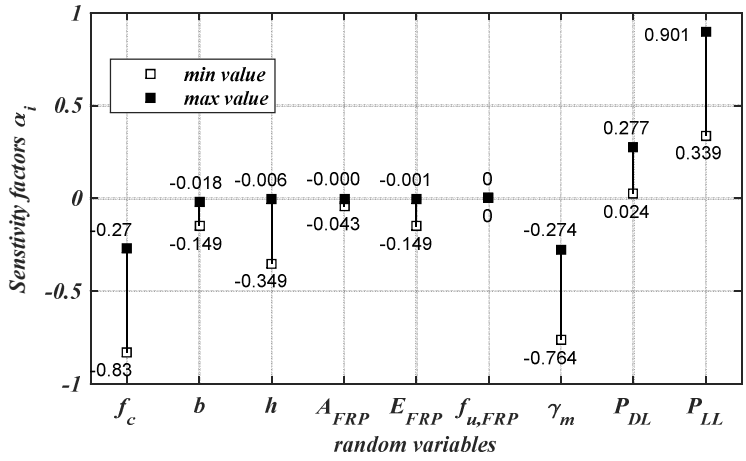

Figure 11. Maximum and minimum values of sensitivity factors α_i of random variables considered (Uniform configuration).

Although FRP ultimate compressive strain will never be reached in concrete columns reinforced with FRP bars as it is controlled by the concrete compressive strain (=0.003), the ACI-440.1R-15 [9] design guide does not recommend relying on FRP bars that carry compressive stresses. Additionally, FIB [10] reports that FRP (or just glass-FRP) bars under compression loads should be ignored unless otherwise stated by experimental studies. Recently, many experimental studies, such as [37, 38, 48-50] have been carried out to study the behaviour of concrete columns reinforced with FRP bars under eccentric compressive forces. All these studies confirm the ability of concrete columns reinforced with FRP bars to efficiently support axial compressive loads with small and high eccentricities. Nevertheless, using glass-FRP bars reduces the column capacity by 13% when compared to an equivalent amount of conventional steel bars, as reported in [49]. However, FRP bars are still more economical than steel bars when a long-life cycle is required, especially in highly corrosive/coastal zones.

To conclude, our article, a working example of the design is proposed to assess the efficiency of the calibrated strength factor in producing FRP-reinforced RC columns with $\beta \geq \beta_T$. A rectangular concrete column with dimensions equal to b=350 mm and h=800 mm is considered. Concrete cover was taken equal to c=25 mm. The results are plotted in Figure 12 in the form of an interaction diagram normalized with respect to the cross-sectional dimension. Different FRP reinforcement ratios (ρ=1,2,3,4 and 5 where $\rho_{FRP}=\rho/100$) were considered. Two different concrete compressive strengths (fc=30 MPa and fc=50 MPa) were considered. Two different grades were used for FRP bars: Grade-I (*i.e.,* E_{FRP}=38.7GPa and $f_{u,FRP}$=629 MPa) and Grade-II (*i.e.,* E_{FRP}=62.7GPa and $f_{u,FRP}$=1236 MPa). As there are no given rules for columns reinforced with FRP bars, strengths ϕP_u and ϕM_u were obtained using ACI-318 recommendations and considering the elastic behaviour of FRP bars until failure. A strength reduction factor of 0.6 was used as proposed in the present study. During the analysis, concrete crushing was observed to be the most frequent failure mode. The FRP

grade has a significant effect only on the cross-section normalized strengths under high eccentricities. However, concrete strength is the most dominant material factor that could greatly affect the column strengths for both small and high eccentricities. Moreover, the reliability index of each of the analysed cases was recorded and found to be in the range of 4.51→5.13 (i.e., greater than the ACI target value (β_T=4).

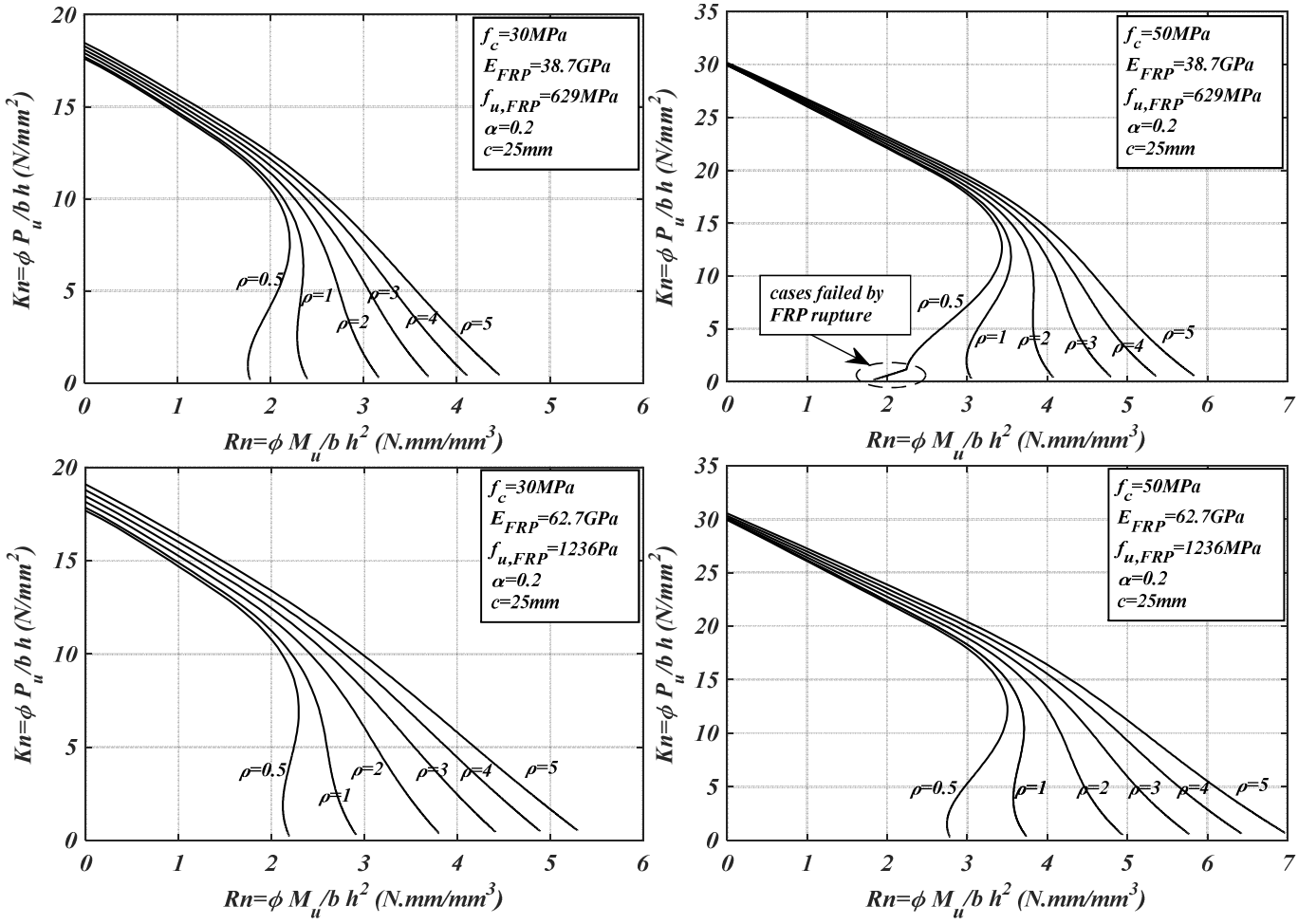

Figure 12. Interaction diagram of concrete sections reinforced with FRP bars (Top-Bottom configuration).

5. Conclusions

Because ACI rules are not addressed for the design of short FRP RC columns, the present study focuses extensively on the probabilistic calibration of the strength reduction factor ϕ, included in the ACI-440 guide, throughout an optimization algorithm. With the objective of providing generalized rules covering most structural classes, approximately 100 000 classes have been considered with two main reinforcement configurations (Top-Bottom and Uniform reinforcement configurations preferred for high- and small-load eccentricities, respectively). In the first step, all design variables (geometrical, loadings, materials) were considered random variables. A fast hybrid first-order reliability

method-based response surface approximation (FORM-RS) and Monte Carlo-based importance sampling (MC-IS) were used to perform the reliability analysis.

Based on this analysis, the first following conclusions can be drawn.

- The concrete crushing failure mode is the most dominant, while FRP rupture occurs in very few design situations and does not exceed 3.5% of the total design situations.
- The strength reduction factor depends mainly on the live-to-dead load ratio and load eccentricity, unlike the FRP strength reduction presented in ACI-440, for the flexural limit state, given by Eq.1.
- A quadratic function of the live-to-dead load ratio and load eccentricity is a more accurate way to specify more accurate values of the strength reduction factor ϕ. This approach with an adjustable value of the reduction factor has proven to be more appropriate for Top-Bottom configurations used in the case of high eccentricity. However, it can be recommended to use a fixed value of ϕ=0.6 for Uniform configurations (case of small eccentricity) to ensure a minimum reliability equal to the target ACI value (β_T=4.0).
- Compression failure can be recommended for FRP-RC columns with Top-Bottom reinforcement configurations, which correspond to high eccentricity values, as FRP-RC columns exhibit a safer design than tension failure columns.
- The strength reduction factor proposed in ACI-440 for designing FRP-RC beams provides an unfeasible design, especially FRP-RC columns with uniform configuration reinforcement.

6. Perspectives

The results obtained in the present study can be considered as an initial guess of the strength reduction factor and the analysis can be extended to include any other expected ranges of the design parameters. In addition, the calibration algorithm developed in the present study can be extended over other code formats such as Euro or Canadian codes. Furthermore, the study can also be used to include other loading configurations (*e.g.* biaxial loading) and/or slender FRP-bars RC columns. Moreover, other secondary effects can be included in the analysis such as confinement effect, bulking of FRP bars, etc.

Data availability statements

Some or all data, models, or code that support the findings of this study are available from the corresponding author upon reasonable request (MATLAB code used for reliability assessment).

References

[1] Y. Zhou, Y Zheng, J. Pan, L. Sui, F. Xing, H. Sun, P. Li, "Experimental investigations on corrosion resistance of innovative steel-FRP composite bars using X-ray microcomputed tomography", *Composites Part B: Engineering*, Vol. 161, pp. 272-284, 2019.

[2] Y. T. Obaidat, A. M. Ashteyat, A. T. Obaidat and S. F. Alfaris. A new technique for repairing reinforced concrete columns. Journal of Building Engineering, vol 30, Article 101256, 2020.

[3] D. Bigaud, O. Ali, "Time-variant flexural reliability of RC beams with externally bonded CFRP under combined fatigue-corrosion actions", *Reliability Engineering & System Safety*, vol. 131, pp. 257–270, 2014.

[4] A. Younis, U. Ebead, P. Suraneni, A. Nanni, "Cost effectiveness of reinforcement alternatives for a concrete water chlorination tank", Journal of Building Engineering, vol. 27, Article 100992, 2020.

[5] A. Veljkovic, V. Carvelli, M.M. Haffke, M. Pahn, "Concrete cover effect on the bond of GFRP bar and concrete under static loading", *Composites Part B: Engineering*, Vol. 124, pp. 40-53, 2017.

[6] B. Kim, J. -Y. Lee, "Resistance of interfacial debonding failure of GFRP bars embedded in concrete reinforced with structural fibers under cycling loads", *Composites Part B: Engineering*, Vol. 156, pp. 201-211, 2019.

[7] A. Siddika, Md. A. Al Mamunb, R. Alyousef and Y.H. M. Amran, "Strengthening of reinforced concrete beams by using fiber-reinforced polymer composites: A review", Journal of Building Engineering, vol. 25, Article 100798, 2019.

[8] A. T. Obaidat, A. M. Ashteyat, S. Hanandeh and A. Y. Al-Btoush, "Behavior of heat damaged circular reinforced concrete columns repaired using Carbon Fiber Reinforced Polymer rope". Journal of Building Engineering", 31, Article 101424, 2020.

[9] ACI-440.1R-15 Committee*: Guide for the Design and Construction of Structural Concrete Reinforced with FRP Bars*. 2015.

[10] Fib Bulletin 40, *FRP reinforcement in RC structures*, Fib Technical Report by Task Group 9.3, 2007.

[11] ISIS Canada, *Reinforcing Concrete Structures with Fibre Reinforced Polymers*, no. 3. 2007.

[12] CAN/CSA S806, "Design and Construction of Building Structures with Fibre-Reinforced Polymers," Canadian Standards Association, Mississauga, Ontario, 2012.

[13] A. Salah-Eldin, H. Mohamed and B. Benmokrane, "Structural performance of high-strength-concrete columns reinforced with GFRP bars and ties subjected to eccentric loads", *Journal of Engineering Structures*, vol 185, pp. 286-300, 2019.

[14] B. Fillmore and P. Sadeghian. Contribution of Longitudinal Glass Fiber-Reinforced Polymer Bars in Concrete

Cylinders under Axial Compression," Canadian Journal of Civil Engineering, vol 45, no. 6, pp 423-525, 2018.

[15] M. Z. Afifi, H. M. Mohamed, and B. Benmokrane. "Axial Capacity of Circular Concrete Columns Reinforced with GFRP Bars and Spirals," Journal of Composites for Construction vol 18, no. 1, Papper ID:04013017, 2014.

[16] A. Hadhood, H. M. Mohamed, F. Ghrib, and B. Benmokrane. "Efficiency of glass-fiber reinforced-polymer (GFRP) discrete hoops and bars in concrete columns under combined axial and flexural loads," Composites Part B, vol 114, pp 223-236, 2017.

[17] K. Khorramian and P. Sadeghian. "Experimental Investigation of Short and Slender Rectangular Concrete Columns Reinforced with GFRP Bars under Eccentric Axial Loads," Journal of Composites for Construction vol 24, no. 6, Paper ID: 04020072, 2020.

[18] CAN/CSA S6, "Canadian Highway Bridge Design Code," Canadian Standards Association, Mississauga, Ontario, 2014.

[19] ACI 318-14 Committee, *Building Code Requirements for Structural Concrete (ACI 318-14)*. 2014.

[20] A. Mohamed, R. Soares, W. S. Venturini, "Partial safety factors for homogeneous reliability of nonlinear reinforced concrete columns", *Structural Safety*, vol. 23, no. 2, pp. 137–156, 2001.

[21] D. M. Frangopol, Y. Ide, E. Spacone, I. Iwaki, "A new look at reliability of reinforced concrete columns," *Structural Safety*, vol. 183, no. 2, pp. 123–150, 1996.

[22] S. M. C. Diniz, D. M. Frangopol, "Safety evaluation of slender high-strength concrete columns under sustained loads", *Computers and Structures*, vol. 81, no. 14, pp. 1475–1486, 2003.

[23] S. A. Mirza, "Reliability-based design of reinforced concrete columns", *Structural Safety*, vol. 18, no. 2–3, pp. 179–194, 1996.

[24] M. Szerszen, A. S. Nowak, "Calibration of design code for buildings (ACI 318): Part 2-reliability analysis and resistance factors", *ACI Structural Journal*, vol. 100, no. 3, pp. 383–391, 2003.

[25] R. A. Atadero, V. M. Karbhari, "Calibration of resistance factors for reliability based design of externally-bonded FRP composites", *Composites Part B: Engineering*, vol. 39, no. 4, pp. 665–679, 2008.

[26] X. Huang, Y. Zhou, F. Xing, Y. Wu, N. Han, "Reliability-based design of FRP flexural strengthened reinforced concrete beams: Guidelines assessment and calibration", *Engineering Structures*, In press, corrected proofAvailable online 22 November 2019. Article 109953

[27] X. Huang, L. Sui, F. Xing, Y. Zhou, Y. Wu, "Reliability assessment for flexural FRP-Strengthened reinforced concrete beams based on Importance Sampling", *Composites Part B: Engineering*, Vol. 156, pp. 378-398, 2019.

[28] M. Coelho, L. Neves, J. Sena-Cruz, "Designing NSM FRP systems in concrete using partial safety factors", *Composites Part B: Engineering*, Vol. 139, pp. 12-23, 2018.

[29] G.P. Lignola, F. Jalayer, F. Nardone, A. Prota, G. Manfredi, "Probabilistic design equations for the shear capacity of RC members with FRP internal shear reinforcement", Composites Part B: Engineering, Vol. 67, pp. 199-208, 2014.

[30] K. Nasrollahzadeh, R. Aghamohammadi, "Reliability analysis of shear strength provisions for FRP-reinforced concrete beams", Engineering Structures, Vol. 176, pp. 785-800, 2018.

[31] Y. Zhou, J. Zhang, W. Li, B. Hu, X. Huang, "Reliability-based design analysis of FRP shear strengthened reinforced concrete beams considering different FRP configurations", Composite Structures, Vol. 237, Article 111957, 2020.

[32] J.R. Casas, J.L. Chambi, "Partial safety factors for CFRP-wrapped bridge piers: Model assessment and calibration", Composite Structures, Vol. 118, pp. 267-283, 2014.

[33] H. Baji, H.R. Ronagh, C.-Q. Li, "Probabilistic assessment of FRP-confined reinforced concrete columns", Composite Structures, Vol. 153, pp. 851-865, 2016.

[34] B. Behnam, C. Eamon, "Reliability-based design optimization of concrete flexural members reinforced with ductile FRP bars", Construction and Building Materials, Vol. 47, pp. 942-950, 2013.

[35] M. Shahnewaz, R. Machial, M.S. Alam, A. Rteil, "Optimized shear design equation for slender concrete beams reinforced with FRP bars and stirrups using Genetic Algorithm and reliability analysis", Engineering Structures, Vol. 107, pp. 151-165, 2016.

[36] Z. Saleh, M. Goldston, A. M. Remennikov and M. N. Sheikh, "Flexural design of GFRP bar reinforced concrete beams: An appraisal of code recommendations", Journal of Building Engineering, vol. 25, Article 100794, 2019.

[37] K. Khorramian and P. Sadeghian. "Experimental and analytical behavior of short concrete columns reinforced with GFRP bars under eccentric loading," *Journal of Engineering Structures*, vol 151, pp. 761-773, 2017.

[38] S. Mirza and B. Skrabek, "Reliability of Short Composite Beam-Column Strength Interaction", *Journal of Structural Engineering*, vol. 117, no. 8, pp. 2320–2339, 1991.

[39] J. Lemaire, M. Chateauneuf, A. Mitteau, *Structural Reliability*. Ed. Wiley, ISBN : 978-1848210820, 508 pages, 2009.

[40] R. C. Soares, A. Mohamed, W. S. Venturini and M Lemaire, "Reliability analysis of non-linear reinforced concrete beams using the response surface method," Journal of Reliability Enineering & System Safety, vol 75, pp 1-16, 2002.

[41] H. Gavin and S. C. Yau, "High-order limit state functions in the response surface method for structural reliability analysis," Journal of Structural Safety, vol 30, pp 162-179, 2006.

[42] X. S. Nguyen, A. Sellier, F Duprat, and G. Pons. “Adaptive response surface method based on a double weight regression technique,” *Journal of Probabilistic Engineering Mechanics*, vol. 24, pp. 135-143, 2009.

[43] S. Chakraborty and A. Sen. “Adaptive response surface based efficient Finite Element Model Updating,” *Journal of Finite Elements in Analysis and Design*, vol. 80, pp. 33-40, 2014.

[44] K. Khorramian and P. Sadeghian. "Material Characterization of GFRP Bars in Compression using a New Test Method," Journal of Testing and Evaluation vol 49, no. 2, pp 1037-1052, 2021.

[45] M. Pilakoutas, K. Neocleous and K. Guadagnini, “Design Philosophy Issues of FRP RC Structures,” *Composites for construction*, vol. 6, no. 3, pp. 154–161, 2002.

[46] N. Gayton, A. Mohamed, J. D. Sorensen, M. Pendola, and M. Lemaire, “Calibration methods for reliability-based design codes,” *Structural Safety*, vol. 26, no. 1, pp. 91–121, 2004.

[47] Matlab R2015a. 2015. Matlab user’ manual.

[48] X. Fan and M. Zhang, "Behaviour of inorganic polymer concrete columns reinforced with basalt FRP bars under eccentric compression: An experimental study," Composites Part B, vol 104, pp. 44-56, 2016.

[49] L. Sun, M. Wei and N. Zhang. Experimental study on the behavior of GFRP reinforced concrete columns under eccentric axial load," Construction and Building Materials, vol 152, pp. 214–225, 2017.

[50] M. Elchalakani and G. Ma. "Tests of glass fibre reinforced polymer rectangular concrete columns subjected to concentric and eccentric axial loading," Engineering Structures, vol 151, pp. 93–104, 2017.

Bibliographical notes

Osama ALI is Assistant Professor in the civil engineering department, faculty of engineering, Aswan University, Egypt. He holds his BSc degree in civil engineering from faculty of engineering, Aswan University. He awarded his MSc degree from structural engineering department, faculty of engineering, Cairo University (Egypt). The thesis entitled: Elastic analysis and Design of Pre-stressed composite girder. He received his PhD from Angers University, France, in 2012. PhD title is: Time-dependent reliability of FRP strengthened reinforced concrete beams under coupled corrosion and changing loading effects. His research activities in the areas of structural reliability of RC structures, finite element analysis of RC structures, strengthening and repair of RC structures using FRP composites, structural optimization, corrosion of steel reinforcement embedded in concrete and performance of RC structures under seismic loads.

Mohamed Zakaria is Associate Professor in the civil engineering department, faculty of engineering, Aswan University, Egypt. He holds his BSc degree in Civil Engineering from faculty of engineering, Aswan University. He awarded his MSc degree from structural engineering department, faculty of engineering, Cairo University (Egypt). His master thesis entitled: Analysis of Prestressed concrete deep beams. He received his PhD from Hokkaido University, Japan, in 2010. PhD title is: Shear cracking behaviour in concrete beams with shear reinforcement. He awarded JSCE Yoshida prize, in 2012. He received postdoctoral fellowship from Japan society for promotion of science (JSPS), Muroran institute of technology, Japan, in 2013, with main target to apply green technology towards general concrete buildings. His research activities in the areas of strengthening and repair of RC structures using FRP composites, construction materials, concrete durability, shear behaviour, structural reliability, finite element modelling and structural performance of RC structures.

Hassen RIAHI Ph.D. in mechanical and civil engineering, is an associate professor at Angers University in France since 2014. His research interests the development of numerical models to solve the problem of the curse of dimensionality frequently encountered in uncertainty propagation though mechanical models. The concerned domains are mainly, fatigue of materials, fracture mechanics and structures subjected to seismic loading.

David BIGAUD is specialized in polymer and composite materials (Eng. 1993 from ITECH-Lyon). He obtained his PhD in 1997 on the topic of the multi-scale modelling of textile-reinforced composite materials. From 1998 to 2005, he was Associate Professor and has developed research on 3D textile-reinforced composites for civil engineering, transportation and aeronautical applications. In September 2005, he was promoted to a position of full Professor at the University of Angers. He develops there in Angers research activities on reliability and decision making about safety of systems. His research has resulted in many publications in several international journals. His research interests are related to the field of civil engineering and with emphasis on structures: pathology, materials, technical management and design of structures.